

# Monitoring of deployment process of shape memory polymers for morphing structures with embedded fibre Bragg grating sensors

Peng Li<sup>1,2</sup>, Zhijun Yan<sup>2</sup>, Lin Zhang<sup>2</sup>, Yanju Liu<sup>3</sup>, Jinsong Leng<sup>1</sup>  
and K.T. Lau<sup>4</sup>

Journal of Intelligent Material Systems  
and Structures

2014, Vol. 25(10) 1224–1232

© The Author(s) 2013

Reprints and permissions:

sagepub.co.uk/journalsPermissions.nav

DOI: 10.1177/1045389X13502875

jim.sagepub.com



## Abstract

This article demonstrates the use of embedded fibre Bragg gratings as vector bending sensor to monitor two-dimensional shape deformation of a shape memory polymer plate. The shape memory polymer plate was made by using thermal-responsive epoxy-based shape memory polymer materials, and the two fibre Bragg grating sensors were orthogonally embedded, one on the top and the other on the bottom layer of the plate, in order to measure the strain distribution in both longitudinal and transverse directions separately and also with temperature reference. When the shape memory polymer plate was bent at different angles, the Bragg wavelengths of the embedded fibre Bragg gratings showed a red-shift of 50 pm/° caused by the bent-induced tensile strain on the plate surface. The finite element method was used to analyse the stress distribution for the whole shape recovery process. The strain transfer rate between the shape memory polymer and optical fibre was also calculated from the finite element method and determined by experimental results, which was around 0.25. During the experiment, the embedded fibre Bragg gratings showed very high temperature sensitivity due to the high thermal expansion coefficient of the shape memory polymer, which was around 108.24 pm/°C below the glass transition temperature ( $T_g$ ) and 47.29 pm/°C above  $T_g$ . Therefore, the orthogonal arrangement of the two fibre Bragg grating sensors could provide a temperature compensation function, as one of the fibre Bragg gratings only measures the temperature while the other is subjected to the directional deformation.

## Keywords

Shape memory polymers, fibre Bragg grating, vector sensors, shape sensing, deployment process

## Introduction

In recent years, a new type of smart materials – shape memory polymers (SMPs) – has been widely developed and used in biomaterials, actuators, sensors and textile applications. SMPs possess some ability to recover to their original shapes after being deformed when exposed to an external stimulus (e.g. heat (Ji et al., 2006), electricity (Sahoo et al., 2007), light (Lendlein et al., 2005), magnetism (Schmidt, 2006) and moisture (Lv et al., 2008)). Comparing with conventional resin-based composites, SMPs have been appreciated as a new generation of functional materials due to their unique material properties, such as large recoverable strain, low density, controllability of recovery behaviour and low cost. With an increasing demand of highly adaptive vehicles for space engineering applications, the shape memory performance of SMPs makes them to meet the requirements for out space missions, and it is also expected to further promote the

development of smart morphing structures, such as deployable space structures and morphing wings for aircraft engineering applications. So far, the study on SMP

<sup>1</sup>Centre for Composite Materials and Structures, Harbin Institute of Technology (HIT), No. 2 YiKuang Street, Harbin, 150080, P.R. China

<sup>2</sup>Aston Institute of Photonic Technologies, School of Engineering & Applied Science, Aston University, Birmingham, B4 7ET, UK

<sup>3</sup>Department of Aerospace Science and Mechanics, No. 92 West DaZhi Street, Harbin Institute of Technology (HIT), Harbin, 150001, P.R. China

<sup>4</sup>Department of Mechanical Engineering, the Hong Kong Polytechnic University, Kowloon, Hong Kong SAR

## Corresponding authors:

Lin Zhang, Aston Institute of Photonic Technologies, School of Engineering & Applied Science, Aston University, Birmingham B4 7ET, UK.  
Email: L.zhang@aston.ac.uk

Jinsong Leng, Centre for Composite Materials and Structures, Harbin Institute of Technology (HIT), No. 2 YiKuang Street, Harbin 150080, P.R. China.

Email: lengjs@hit.edu.cn

space deployable structures is mostly focused on the fundamentals, design, fabrication, modelling and characterization and stimulus methods (Mark et al., 2001; Yee et al., 2004). A few studies (Li et al., 2013) have been carried out on the monitoring and controlling of the shape recovery deformation process of morphing structures based on SMPs. In the out space environment, the deployable process of the morphing structures could not be directly observed. So it is very important to develop a structural health monitoring method to directly or indirectly monitor and detect the deformation process of the morphing structures based on SMPs to ensure their safety in operation.

A number of non-contact methods, including the charge-coupled device (CCD) camera measurement system (Chan et al., 2009), the laser scanning measurement system (Anand et al., 2009), laser holography and measurements from photographs (Babovsky et al., 2011), were previously used to measure the deformation of structures. These methods can be applied for whole field measurements in all structures. However, physical controlling and data acquisition systems must be installed somewhere close to the structure; thus, it is not suitable for real-time monitor at out space environment. On the other side, some contact techniques have been proposed to monitor the shape and health condition of morphing structures by using fibre optic sensors. Nishio et al. (2010) used Brillouin-scattering-based optical fibre sensors for structural shape reconstruction; Rapp et al. (2009) investigated the reconstruction method of structural deformation of two-dimensional (2D) structures by using a displacement-strain-transformation matrix and Bragg grating sensors. However, fibre sensors are used for only detecting strain in these measurements; thus, they require complex algorithms and models to measure the shape deformation.

Fibre Bragg grating (FBG) sensors (Calabro et al., 2007; Fernando et al., 2003; Leng and Asundi, 2003) have been widely accepted as excellent sensors for structural health monitoring, due to their small physical size which can be easily embedded into a structure without inducing any harmful effect, well-developed integration technique which is possible to achieve wireless sensing network, fast response time and immunity to electromagnetic interference, all of these making them very suitable for environment and structure health monitoring under different conditions. This article presents the feasibility study of using embedded FBG sensors to measure the bent-induced deformation of an SMP plate subjected to shape memory action. The dynamic shape recovery of a 2D SMP structure was monitored by two FBG sensors that were embedded orthogonally into the SMP plate.

## Theoretical background

### Deformation and recovery process of the SMP plate

An active morphing deformation process of an SMP structure which involves a thermo-mechanical cycle of

the shape fixing and recovery is shown in Figure 1. The shape deformation and recovery process is described as following: firstly, the SMP plate is heated up above its glass transition temperature ( $T_g$ ) and bent to  $180^\circ$  by rolling it on a cylinder with the radius of 3 cm; then, the sample is cooled down to the room temperature while maintaining its bending shape; finally, the SMP plate is heated again above its  $T_g$  and during this process the SMP plate is naturally recovered back to the initial flat shape and completes 1 cycle of the structure deformation and recovery.

If the FBG vector sensors are embedded in the SMP plate, the deformation and recovery of the SMP plate can be monitored at any position ( $\theta$ ) by measuring the bent-induced Bragg wavelength changes of the two embedded FBG vector sensors. In the experiment, the SMP plate was bent to a desirable angle above its  $T_g$  and then cooled down to keep its shape at room temperature. The deformation of the SMP plate was assumed under a pure bending condition, then it can be regarded that the bent-induced strain is constant over the whole structure.

### Sensing principle

In principle, once the SMP plate is deformed, the embedded FBG sensors will experience the bent-induced strain  $\varepsilon_m$ , but this strain is smaller than the bent-induced actual strain  $\varepsilon$  in the SMP plate, because the FBGs and the SMP plate are made of two different materials with different thermal expansion coefficients. Thus, the strain experienced by the FBG  $\varepsilon_m$  should be the product of the real strain  $\varepsilon$  induced by structure deformation and the strain transfer rate  $\kappa$ , which is expressed as

$$\varepsilon_m = \kappa \varepsilon \quad (1)$$

The strain transfer rate  $\kappa$  is depending on various parameters, such as mechanical and geometric properties of the SMP, coating material on the fibre, thickness of the FBG sample and embedded length of the fibre. Because at high temperature, the thermal expansion coefficient and elastic modulus of the SMP are much larger than that of the silica fibre glass, the strain transfer rate  $\kappa$  will be very small at high temperature; thus, the FBG will experience much smaller strain than the SMP plate. To monitor the curing and deformation processes of the SMP plate, it requires the measurements of both temperature and stress quantities. FBG sensors exhibit dual sensitivity since their Bragg wavelength shift depends on the change of either applied strain or temperature; the shift can be calculated by the following equation (Kersey et al., 1997)

$$\frac{\Delta\lambda_B}{\lambda_B} = s_\varepsilon \Delta\varepsilon + s_T \Delta T \quad (2)$$

where  $s_\varepsilon$  is the strain coefficient, which is related to the strain-optic properties of the fibre and  $s_T$  is the

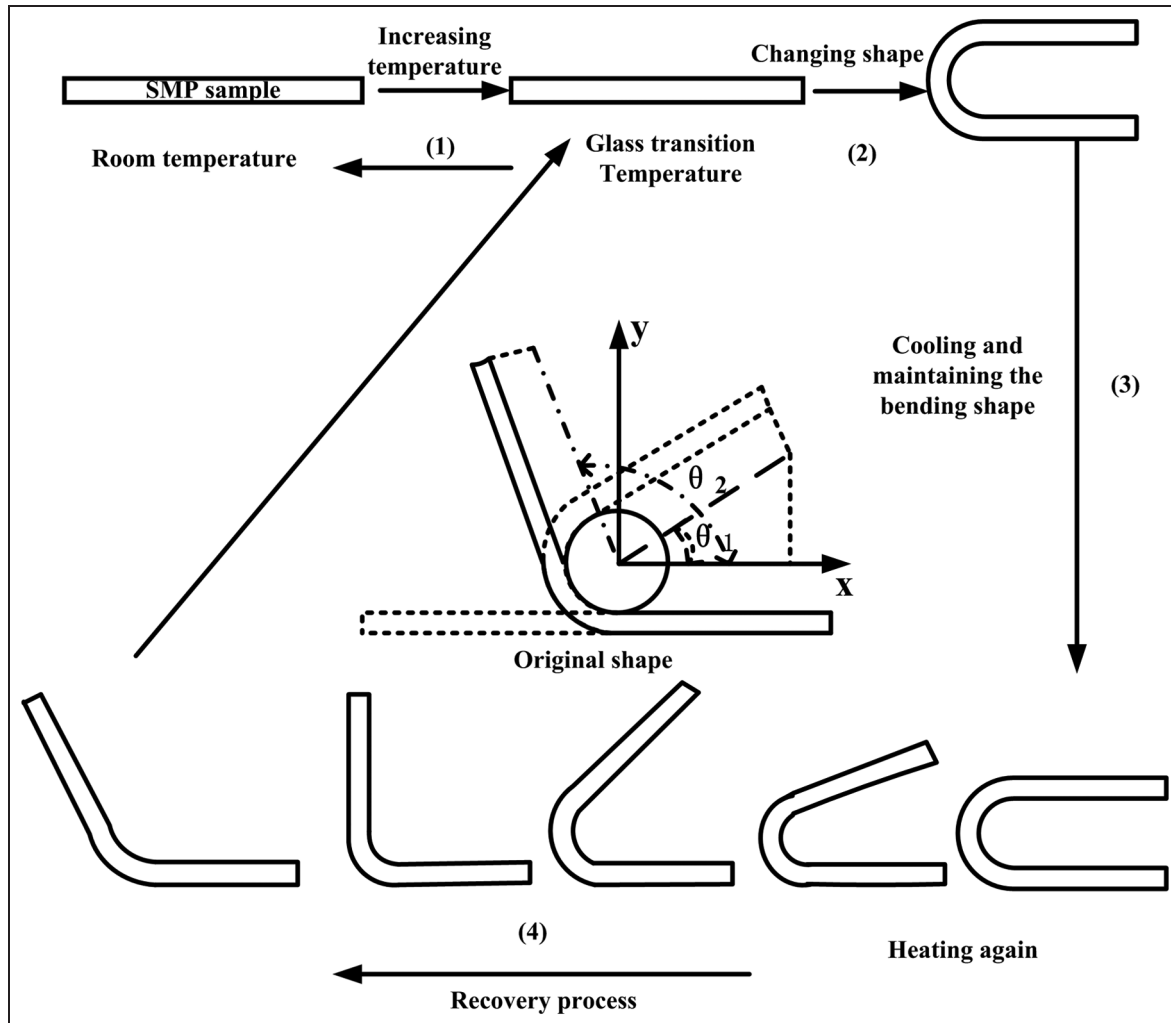


**Figure 1.** The schematic of the actively deforming and recovering process of a morphing SMP structure during a typical thermo-mechanical cycle.

SMP: shape memory polymer.

temperature coefficient, which is contributed by the thermal-expansion and the thermo-optic effects of the fibre. If the strain- and temperature-induced Bragg wavelength shifts can be discriminated, it is then possible to measure simultaneously both temperature and strain. The proposed fibre optic measurement system consists of two FBG sensors which are embedded into the SMP plate orthogonally on the top and bottom surface; thus, in this arrangement, one FBG can be used as temperature reference sensor, while the other is experiencing directional bending along its fibre axis direction.

## Experimental tests

### SMP material

A new type of thermal-responsive epoxy-based SMP was employed for the experiment, which is a potential

material for outer space structure application. This amorphous epoxy-based SMP contains stable chemical functional groups and has a good viscoelasticity and its shape memory effect can be triggered by heat. The epoxy-based SMP can be deformed to any desired shape at the temperature above its glass transition temperature ( $T_g$ ). Equally, at or above its  $T_g$ , the SMP can quickly and completely recover back to the initial shape, which shows a good shape memory effect. The shape memory properties make the epoxy-based SMP show two phases: frozen and reversible phase. The former is responsible for memorizing the original shape and usually achieved via chemical or physical cross-linking (e.g. chain entanglement and crystallization) and the latter corresponds shape change under stimulus. The  $T_g$  (about  $100^\circ\text{C}$ ) determined by differential scanning calorimetry (DSC) and thermal decomposition temperature is high enough for the application in aerospace morphing structures fields. Meanwhile, the

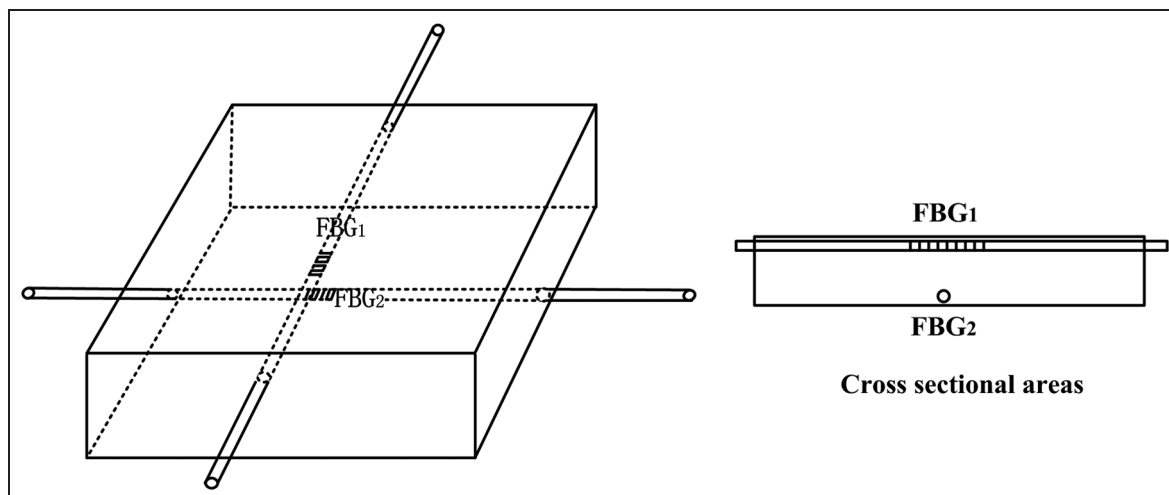


**Figure 2.** The SMP plate and arrangement of the two embedded FBG sensors.  
SMP: shape memory polymer; FBG: fibre Bragg grating.

SMP material possesses high elastic modulus (3 GPa) and strength (40–50 MPa) at the room temperature (Lan et al., 2009). Furthermore, according to its mechanical property, this epoxy-based SMP is consistent with standard engineering plastics and can be used as aerospace structural material.

### Preparation of the FBG sensors

The FBG sensors were ultraviolet (UV)-inscribed in hydrogen loaded standard single mode telecom fibre (SM-28) using a frequency doubled Ar ion laser with the standard phase mask scanning technique. A total of two FBGs of 1 mm length with Bragg wavelengths at 1558 and 1552 nm were UV-inscribed into the fibre. The short length grating was chosen to avoid the spectral split effect caused by un-uniform stress. After UV inscription, the FBGs were annealed at 150°C for 48 h to stabilize their property at high operation temperature. Finally, in order to maintain the durability, the stripped grating areas on the fibre were recoated using acrylic resin.

### SMP sample manufacturing and sensor embedding

The polymer matrix for the SMP was composed of epoxy-based resin, hardener and an active linear epoxy monomer. The resin and hardener were mixed with a weight ratio of 1:1. An active linear epoxy monomer content of 5 wt% was co-polymerized with the polymer matrix to adjust its molecular structure. The structure of the SMP matrix is known to be a thermoset cross-linked network, and the composition and preparation of the epoxy-based SMPs have been reported in previous study (Leng et al., 2009).

The pre-polymer mixture was degassed in a vacuum oven at 50°C to obtain a bubble-free pre-polymer.

A rectangular aluminium mould with dimensions of  $60 \times 60 \times 2 \text{ mm}^3$  was designed to inject SMP polymer solution to form the plate. A total of four tiny passages were made to allow optical fibres to pass through and maintain straight at pre-designed positions. The aluminium mould was cleaned with alcohol and a thin coating of Teflon facecloth was applied on to the surface. A total of two optical fibres containing the two FBG sensors were laid on the mould in orthogonal directions and one was placed close to the internal top surface and the other to the internal bottom surface of the mould and then were slightly pre-strained to avoid any compressive load, buckling and misalignment of the fibre during the embedding processing. The pre-polymer solution was then injected into the mould. A three-step thermal cure process was performed for the pre-polymer at first 80°C for 3 h, then at 100°C for further 3 h and finally at 150°C for 5 h. To stabilize the properties of the SMP plate, the plate was annealed at 180°C for 3 h after being removed from the mould. Figure 2 shows the structure schematic of the SMP plate embedded with two FBG sensors.

## Experimental results and discussion

### FBG spectra before and after embedding

The transition spectra of the two embedded FBG sensors were monitored for pre, during and after the embedding using a broadband light source and an optical spectrum analyser with a resolution of 0.05 nm. Figure 3 shows the evolving spectra for one of the FBGs (FBG<sub>1</sub> with initial Bragg wavelength at 1558 nm). The three peaks shown in Figure 3 correspond to pre-cured, after-cured and after-annealed processes when the SMP plate was kept in a flat position at room temperature (25°C). It is seen from the figure that the

Bragg resonance has blue-shifted by  $\sim 6.5$  nm from the pre-cured to after-cured (embedded) stage and further  $\sim 8.5$  nm after annealing. The blue-shifts indicate that during the embedding and annealing processes, there was a compressive strain superimposed to the FBG sensors, as a consequence of the consolidation of the pre-polymer from high temperature to room temperature.

### FBG response to shape deformation

In order to quantitatively analyse the bending-induced shape deformation or recovery of the SMP plate at the temperature above its  $T_g$ , the responses of FBG<sub>1</sub> and FBG<sub>2</sub> were monitored when the SMP plate was

subjected to the bending. The bending experiment was performed as described in the following. Initially, the SMP plate was heated up to  $120^\circ\text{C}$  ( $T_g + 20^\circ\text{C}$ ) to be softened, then the SMP plate was bent to different angles by rolling it on a cylinder with 3 cm radius. The SMP plate was first bent in the direction along the FBG<sub>1</sub> fibre and then to the orthogonal direction along the FBG<sub>2</sub> fibre. Various static conditions for different angles were fixed when the SMP plate cooled down to the room temperature. Figure 4(a) shows the transmission spectra of FBG<sub>1</sub> when the SMP plate was bent at  $0^\circ$ ,  $30^\circ$ ,  $60^\circ$ ,  $90^\circ$ ,  $120^\circ$ ,  $150^\circ$  and  $180^\circ$ . It is seen clearly that the Bragg wavelength shift responses to the seven static angles are corresponding to seven frozen strains. The Bragg wavelength has a red-shift with increasing bending angles. Figure 4(b) shows the relationship between the wavelength shift and frozen deformation angle for FBG<sub>1</sub>, from which it is easy to see that the Bragg wavelength shift exhibits a linear relationship with the bending angle change of the plate and the gradient is measured as around  $50 \text{ pm}/^\circ$ .

Then, the relation between the strain and bending angle was investigated from both experimental measurement and numerical calculation using finite element method (FEM). The comparative results are shown in Figure 5. A 2D finite element (FE) model of the rectangular SMP plate with the dimension of  $60 \times 60 \times 2 \text{ mm}^3$ , elastic modulus of 14.32 MPa and Poisson's ratio of 0.35 was developed. The FE model was conducted using the ABAQUS. In this model, the deformation of the SMP plate was performed by bending one end of the SMP plate while the other end was fixed. The strain values from the FEM method were obtained by post-process of ABAQUS software. It can be seen that both the FEM and experimental results related to

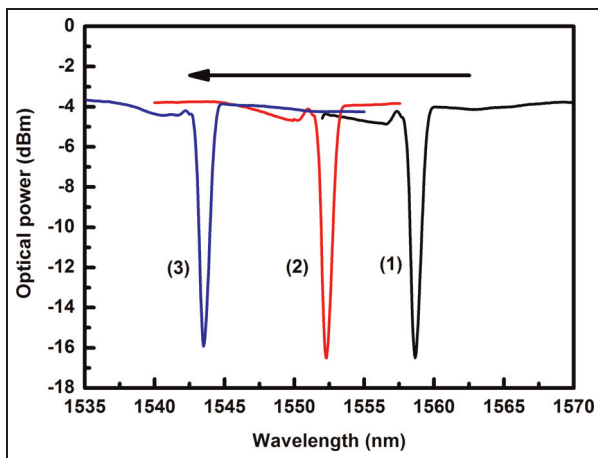


**Figure 3.** The transition spectra of FBG<sub>1</sub> when the SMP sample is in flat shape at room temperature in three different situations: (1) pre-cured, (2) after cured and (3) after annealed. SMP: shape memory polymer; FBG: fibre Bragg grating.

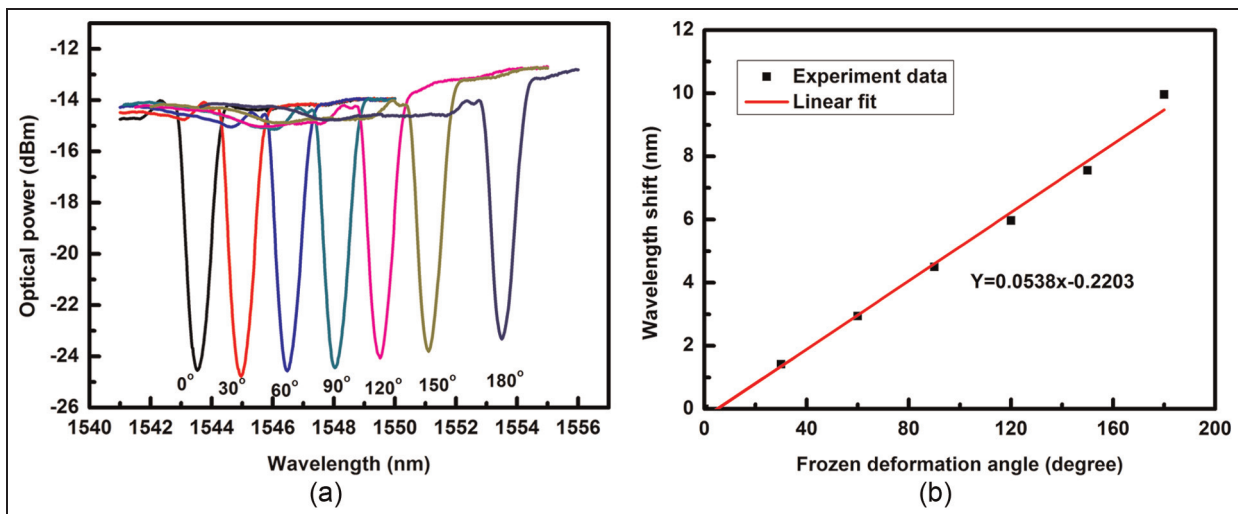


**Figure 4.** (a) The transition spectra and (b) the relation between the Bragg wavelength shift and the bending angle for the FBG<sub>1</sub> embedded to the SMP. SMP: shape memory polymer; FBG: fibre Bragg grating.

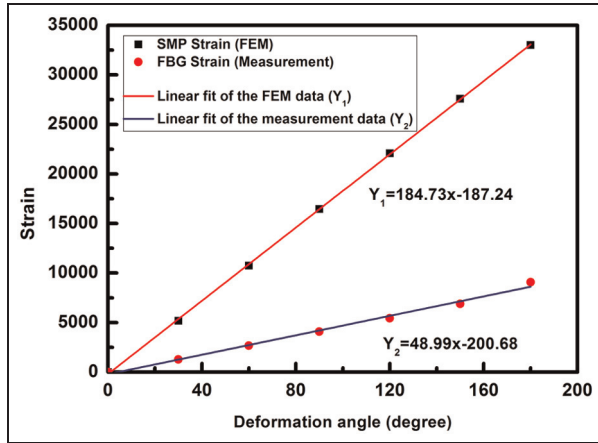


**Figure 5.** The simulated strains using FEM and measured from FBG<sub>1</sub> in relation to deformation angle when the SMP plate was under bending.

FEM: finite element method; SMP: shape memory polymer; FBG: fibre Bragg grating.

the strain increase linearly with the increasing deformation angle, but the simulated strain from FEM is much larger than FBG measured (see Table 1). The FEM analysis just simulated the true strain  $\varepsilon$  produced by assuming the SMP plate was under ideal bending situation at constant temperature 100°C (SMP  $T_g$ ). The FE model takes into account an elastic material model and linear elastic deformations, both tending to provide an over-stiff mechanical response to the SMP plate.

However, the strain sensing performed by the FBG could be affected by the embedding conditions (thickness of sample and embedded length of the fibre), and the characteristics of the interlayer (cladding layer) and the matrix (SMP materials). Thus, when the FBG sensor was embedded into the SMP plate, the FBG experienced strain  $\varepsilon_m$  is smaller than the true strain  $\varepsilon$  induced by the bending on the SMP plate. This is why we see the simulated strain is much higher than the FBG measurement under the same deformation angle in Figure 5.

### Thermal response of embedded FBG sensors

Due to relatively high thermal expansion coefficient of the SMP, thermal strain would be induced during the

shape deformation process. Therefore, it is necessary to have a temperature reference sensor to detect thermal and thermal-mechanical strains separately on the SMP plate. One of the orthogonally embedded FBGs in the SMP plate can provide temperature reference for the other. In the experiment, we first evaluated the temperature effect on the embedded FBG at below and above the SMP  $T_g$ . The temperature effects on FBG<sub>1</sub> at free-standing condition and embedded in the SMP plate were characterized in the temperature range 15°C–135°C. As shown in Figure 6, for the free-standing FBG<sub>1</sub>, it has exhibited a temperature sensitivity of 12.2 pm/°C, while the embedded FBG<sub>1</sub> has shown a much more increased temperature sensitivity 108.24 pm/°C when subjected to the temperature elevation from 15°C to the  $T_g$  100°C and reduced to 47.29 pm/°C from  $T_g$  to 135°C. In comparison, the temperature sensitivity of the embedded FBG<sub>1</sub> has increased around 9 times from the free-standing FBG<sub>1</sub> below the  $T_g$ .

### 2D sensing using two orthogonally embedded FBG sensors

For large space deployable structure, the deformation is much more complicated; thus, the monitoring in multiple directions may be necessary to obtain exactly the shape recovery degree and displacement. In principle, more FBGs may be embedded into the SMP structure forming 2D or three-dimensional (3D) sensor network. In order to evaluate the sensing capability of the two FBGs embedded orthogonally in the SMP plate, we have performed the bending experiment on the SMP plate in two dimensions. Figure 7(a) and (c) shows the bending-induced spectrum changes of FBG<sub>1</sub> and FBG<sub>2</sub>, respectively. Clearly, we can see that when the SMP plate is bent along the FBG<sub>1</sub> fibre direction, only FBG<sub>1</sub> will respond to the bending and its Bragg wavelength shift towards the longer wavelength side, while the FBG<sub>2</sub> remains unchanging as it is not subjected to bending, and vice versa. The actually measured Bragg wavelength shifts against frozen deformation angle for FBG<sub>1</sub> and FBG<sub>2</sub> are plotted in Figure 7(b) and (d), respectively. Quantitatively, we see from Figure 7(b) that when the bending was performed on FBG<sub>1</sub> and the angle changed from 0° to 120°, the FBG<sub>1</sub> has

**Table 1.** The comparison between the FEM simulation and the FBG measurement results.

Deformation angle (°)	FEM stress (Pa)	FEM strain ( $\mu\varepsilon$ )	Measurement results strain ( $\mu\varepsilon$ )	Strain transfer rate
0	0	0	0	0
30	81310.6	5179.9	1293	0.2496
60	173,847	10,748	2677	0.2491
90	267,534	16,463	4098	0.2489
120	358,830	22,083	5437	0.2462
150	448,199	27,589	6885	0.2495
180	536,493	33,008	9071	0.2748

FEM: finite element method; FBG: fibre Bragg grating.

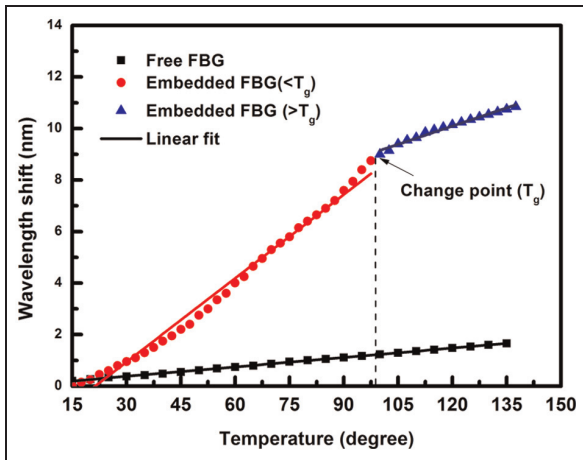


**Figure 6.** Temperature-induced Bragg wavelength shifts of  $FBG_1$  when free standing and embedded in the SMP plate for a temperature range from  $15^\circ\text{C}$  to  $135^\circ\text{C}$ .

SMP: shape memory polymer; FBG: fibre Bragg grating.

red-shifted by  $5.97\text{ nm}$  with a rate of  $0.05\text{ nm/degree}$ , while  $FBG_2$  remained unchanged. Similarly from Figure 7(d), we see that when the bending performed on  $FBG_2$ , its wavelength is shifted by  $5.78\text{ nm}$  with a slightly lower rate at  $0.048\text{ nm/}^\circ$ , while  $FBG_1$  remained almost unchanged. Table 2 lists the exact wavelength shifts and calculated strains from strain–stress relation for  $FBG_1$  and  $FBG_2$  when the 2D bending was performed for bending angles of  $0^\circ$ ,  $30^\circ$ ,  $60^\circ$ ,  $90^\circ$  and  $120^\circ$ .

### Dynamic monitoring of two FBG sensors

The two orthogonally embedded FBGs in the SMP plate can form dynamic sensing monitoring both shape deformation and temperature. We have examined the dynamic response of the embedded FBG sensor when the SMP plate shapes under recovery at the temperature higher than its  $T_g$ . In the experiment, the SMP

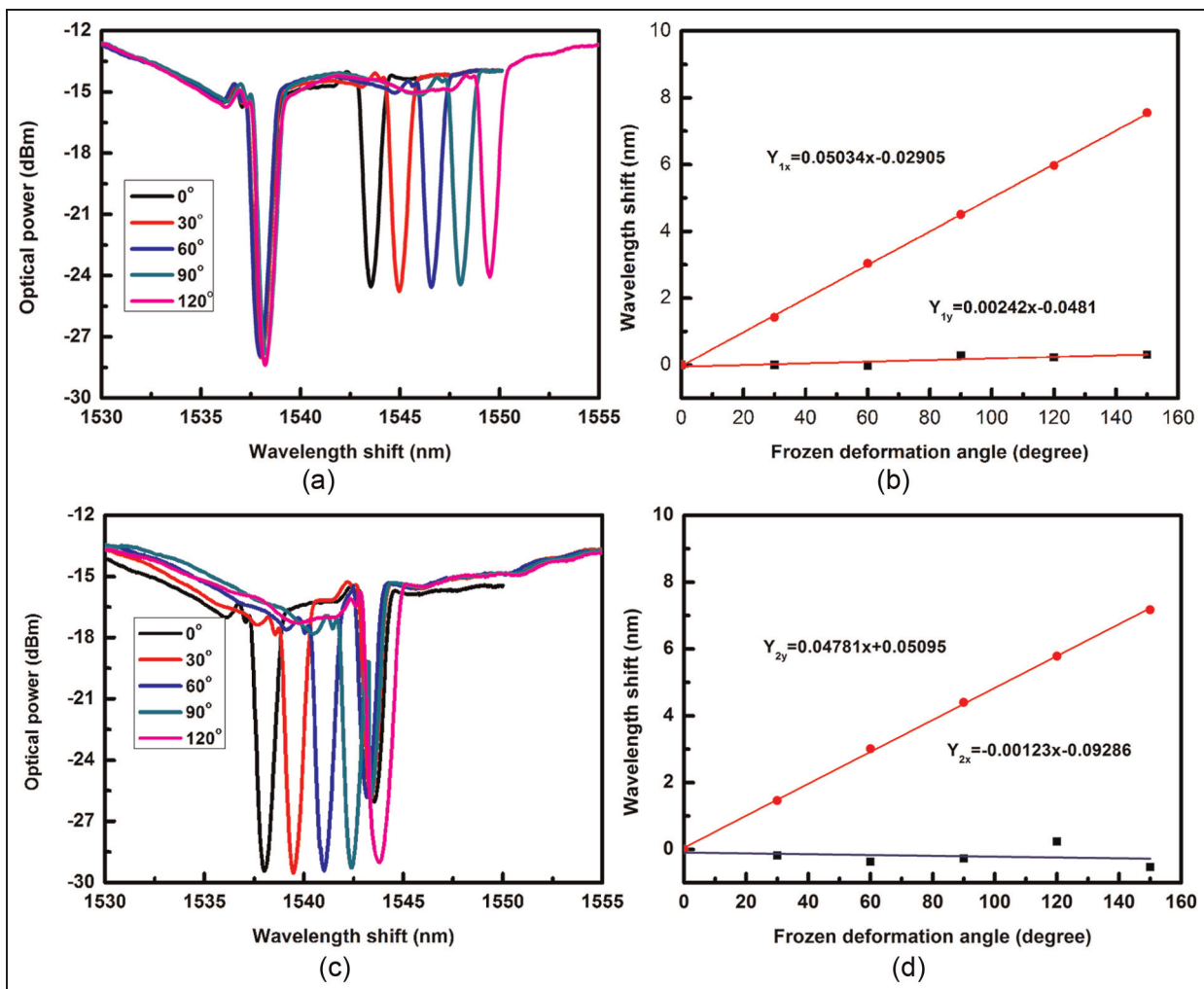


**Figure 7.** The transition spectra of (a)  $FBG_1$  and (c)  $FBG_2$  when the bending is performed on  $FBG_1$  and  $FBG_2$  fibre directions, respectively. The Bragg wavelength shift against frozen deformation angle for (b)  $FBG_1$  and (d)  $FBG_2$  when the SMP plate was bent along  $FBG_1$  and  $FBG_2$  fibre directions, respectively.

SMP: shape memory polymer; FBG: fibre Bragg grating.

**Table 2.** The relation between the mechanical strain and bend angle.

Bending angle (°)	$\Delta\lambda$ (FBG <sub>1</sub> ) (nm)	Strain (FBG <sub>1</sub> ) ( $\mu\epsilon$ )	$\Delta\lambda$ (FBG <sub>2</sub> ) (nm)	Strain (FBG <sub>2</sub> ) ( $\mu\epsilon$ )
0	0	0	0	0
30	1.42	1293.26	1.46	1321.26
60	3.04	2768.67	3.01	2723.98
90	4.5	4098.36	4.4	3981.90
120	5.97	5437.15	5.78	5230.76

FBG: fibre Bragg grating.

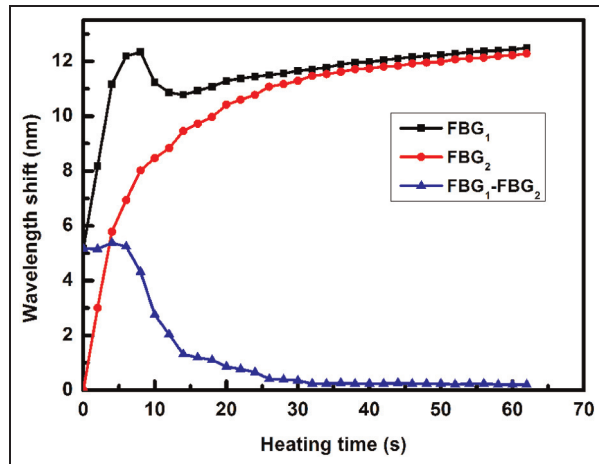


**Figure 8.** The wavelength shifts of the two embedded FBG<sub>1</sub> and FBG<sub>2</sub> sensors during the dynamic process of the shape recovery at the first 60 s in an oven at 120°C.

FBG: fibre Bragg grating.

plate was heated to 120°C and it was bent to 90° through rolling on the cylinder with 3 cm radius. The shape of the deformation was fixed by cooling down the SMP plate to room temperature while maintaining the bent shape at 90°. For this process, the wavelength of both FBGs was shifted almost 5 nm which represent the frozen strain. Then, the deformed SMP plate was put into an oven which had a temperature set at 120°C and the shape recovery process was monitored. The Bragg wavelength responses of both embedded FBGs were measured for 60 s and the wavelength shifts are plotted in Figure 8. It can be seen clearly from the figure that FBG<sub>1</sub> experienced both the temperature and strain effects as the SMP plate was bent along FBG<sub>1</sub> fibre direction, whereas the orthogonal FBG<sub>2</sub> only showed the temperature effect. The triangle point curve is representing the pure strain effect on FBG<sub>1</sub> as the temperature contribution has been compensated by subtracting effect from the FBG<sub>2</sub>. It can also be seen from Figure 8 that the shape recovery was almost completed in the first 30 s as we see the dynamic changes are almost stopped after 30 s, reaching more stable status for both FBG<sub>1</sub> and FBG<sub>2</sub> sensors.

## Conclusion

A simple and practical scheme for shape recovery deformation monitoring of SMP deployable structure model has been demonstrated based on the measurement of two FBG vector sensors embedded orthogonally in the SMP structure. The SMP sample under various static bending angles and dynamic shape recovery deformation processes were investigated. The experimental results clearly showed that the static and dynamic shape recovery deformation of such an SMP deployable structure can be effectively monitored by the embedded FBG sensors. The presented sensing method is easily expandable and can be used as a sensor network for monitoring larger scale 2D shape recovery processes. These attractive physical and operational characteristics are ideally suited for real-time measurement in the out space deployment structure. Although this very first experiment has only used two FBG sensors for proof-of-concept, it should be possible to embed FBG arrays in two dimensions to monitor large-scale deformation of SMP deployable structure in dynamic condition, which will be the further work for the authors.

## Declaration of conflicting interests

The authors declared no potential conflicts of interest with respect to the research, authorship, and/or publication of this article.

## Funding

This project was supported by the research grant of the Harbin Institute of Technology, Aston University and The Hong Kong Polytechnic University Grant.

## References

- Anand A, Chhaniwal VK, Almoró P, et al. (2009) Shape and deformation measurements of 3D objects using volume speckle field and phase retrieval. *Optics Letters* 34(10):1522–1524.
- Babovsky H, Grosse M, Buehl J, et al. (2011) Stereophotogrammetric 3D shape measurement by holographic methods using structured speckle illumination combined with interferometry. *Optics Letters* 36(23):4512–4514.
- Calabro AM, Mazzola L and Caneva C (2007) Integrated sensor system for smart materials: multidisciplinary approach

- using COTS optic fiber sensors. Design, validation and calibration in aeronautical components area. *Proceedings of SPIE* 6530: 65301U-1.
- Chan THT, Ashebo DB, Tam HY, et al. (2009) Vertical displacement measurements for bridges using optical fiber sensors and CCD cameras – a preliminary study. *Structural Health Monitoring* 8(3): 243–249.
- Fernando GF, Hameed A, Winter D, et al. (2003) Structural integrity monitoring of concrete Structures via optical fiber sensors: sensor protection systems. *Structural Health Monitoring* 2(2): 123–135.
- Ji F, Zhu Y, Hu J, et al. (2006) Smart polymer fibers with shape memory effect. *Smart Materials and Structures* 15(6):1547–1554.
- Kersey AD, Davis MA, Patrick HJ, et al. (1997) Fiber grating sensors. *Journal of Lightwave Technology* 15(8): 1442–1463.
- Lan X, Liu Y, Lv H, et al. (2009) Fiber reinforced shape memory polymer composite and its application in a deployable hinge. *Smart Materials and Structures* 18(2):024002.
- Lendlein A, Jiang H, Jünger O, et al. (2005) Light-induced shape-memory polymers. *Nature* 434: 879–882.
- Leng J and Asundi A (2003) Structural health monitoring of smart composite materials by using EFPI and FBG sensors. *Sensors and Actuators A: Physical* 103: 330–340.
- Leng JS, Wu XL and Liu YJ (2009) Effect of a linear monomer on the thermomechanical properties of epoxy shape-memory polymer. *Smart Materials and Structures* 18(9): 095031.
- Li P, Yan Z, Zhou K, et al. (2013) Monitoring static shape memory polymers using a fiber Bragg grating as a vector-bending sensor. *Optical Engineering* 52(1): 014401.
- Lv H, Leng J, Liu Y, et al. (2008) Shape-memory polymer in response to solution. *Advanced Engineering Materials* 10(6): 592–595.
- Mark SL, Naseem AM and Michael LT (2001) Application of elastic memory composite materials to deployable space structures. *AIAA Student Journal: American Institute of Aeronautics and Astronautics* 01(4602): 110.
- Nishio M, Mizutani T and Takeda N (2010) Structural shape reconstruction with consideration of the reliability of distributed strain data from a Brillouin-scattering-based optical fiber sensor. *Smart Materials and Structures* 19: 03501.
- Rapp S, Kang L-H, Han J-H, et al. (2009) Displacement field estimation for a two-dimensional structure using fiber Bragg grating sensors. *Smart Materials and Structures* 18: 025006.
- Sahoo NG, Jung YC and Cho JW (2007) Electroactive shape memory effect of polyurethane composites filled with carbon nanotubes and conducting polymer. *Materials and Manufacturing Processes* 22: 419–423.
- Schmidt AM (2006) Electromagnetic activation of shape memory polymer networks containing magnetic nanoparticles. *Macromolecular Rapid Communications* 27: 1168–1172.
- Yee JCH, Soykasap O and Pellegrino S (2004) Carbon fibre reinforced plastic tape springs. In: *Proceedings of the 45th AIAA/ASME/ASCE/AHS/ASC structures, structural dynamics and materials conference*, Palm Springs, California, CA, 19–22 April, paper no. AIAA 2004-1819.